ACS Macro Letters

Letter

pubs.acs.org/macroletters

Perpendicularly Oriented Block Copolymer Thin Films Induced by Neutral Star Copolymer Nanoparticles

Seyong Kim,[†] Misang Yoo,[†] Julia Baettig,[‡] Eun-Hye Kang,[§] Jaseung Koo,[∥] Youngson Choe,[⊥] Tae-Lim Choi,[§] Anzar Khan,[‡] Jeong Gon Son,*[,#] and Joona Bang*[,†]

[†]Department of Chemical and Biological Engineering, Korea University, Seoul 136-713, Republic of Korea

[‡]Department of Materials, ETH-Zürich, CH-8093 Zürich, Switzerland

[§]Department of Chemistry, Seoul National University, Seoul 151-747, Republic of Korea

[∥]Neutron Science Division, Korea Atomic Energy Research Institute (KAERI), Daejeon, 305-353, Republic of Korea

[⊥]Department of Chemical Engineering, Pusan National University, Kumjeong-ku, Busan 609-735, Republic of Korea

[#]Photo-Electronic Hybrids Research Center, Korea Institute of Science and Technology (KIST), Seoul 136-791, Republic of Korea

Supporting Information

ABSTRACT: By introducing neutral star copolymers consisting of poly(styrene-*r*-methyl methacrylate) (PS-*r*-PMMA) arms, a perpendicular orientation of PS-*b*-PMMA microdomains in thin films could be achieved without any surface treatment. The star copolymers were synthesized by arm-first method in which short chain arms are cross-linked by employing a multifunctional coupling reagent via atom transfer radical polymerization. To find the optimal neutral composition for the perpendicular orientation, we varied the composition of MMA in PS-*r*-PMMA arms from 40 mol % to 80 mol %. It was found that the star copolymer having an overall PS and PMMA composition of 59:41 exhibits the well-ordered perpendicular orientation of lamellar structures after thermal annealing. Furthermore, we also prepared the deuterated star copolymers to trace them within PS-*b*-PMMA films along vertical direction by neutron reflectivity. In this case, it was observed that star copolymers were mainly located at the top surface and bottom interface of the films, thereby effectively neutralizing the surface/interfacial energy differences.

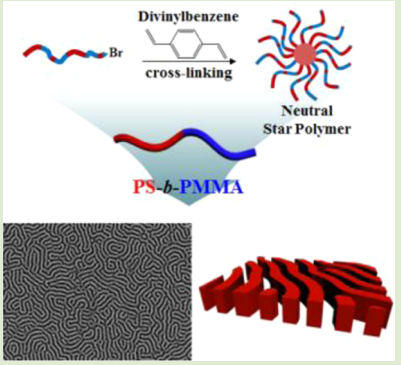

The self-assembly of block copolymers (BCPs) has been considered as one of promising solution to fabricate nanometer scale structures that can overcome the limitations of conventional top-down approaches.[1,2] Many researchers have demonstrated that BCP thin films have great potential to a wide range of applications including templates for nanolithography, microelectronics, separation membranes, and biosensors.[3−7] In many cases, it is desirable that the BCP microdomains are oriented perpendicular to the bottom surface. However, during the self-assembly process of BCP thin films, surface and interfacial energy minimization is enthalpically favorable and thus it is general that one of the blocks in BCPs having lower surface/interfacial energy preferentially wet the air-surface/substrates, resulting in parallel orientation of BCP thin films.[8,9] Therefore, in order to achieve the vertical orientation of BCP microdomains, diverse approaches such as solvent annealing,[10,11] electric field,[12] and rough substrate[13,14] has been suggested, but the random copolymer approach that neutralize the substrate has been dominantly used to obtain the perpendicular orientation of BCP thin films.[15−18]

Recently, the neutralization strategy was further extended to tailoring top surface properties using removable top coats,[19,20] which can enlarge the choice of BCP to achieve the perpendicular orientation using neutralizing materials within BCP films[21] or molecular transfer printing of the nanopatterns.[22] In a similar context, we also demonstrated that an incorporation of surface-tailored Au nanoparticles (NPs) can control the orientation of BCP microdomains.[23] In this system, it was observed that the neutral Au NPs are mainly located at top and bottom surfaces within BCP thin films to reduce the entropic penalty of the BCP chains. As a result, the segregated Au NPs could effectively neutralize the surface and the bottom interface of BCPs, resulting in the perpendicular orientation of BCP microdomains.[24] Although such functions of Au NPs in nanocomposite systems are interesting in both scientific and practical aspects, a use of metal nanoparticles might be obstacles when the BCP templates need to be transferred via lithographic process. In this regard, a star polymer is one of the candidates that can replace the Au NPs due to its comparable size and similar structure; cross-linked core and highly grafted arms, tunability of chemical properties by varying the components and compositions in arms, and most of all, star polymers are composed of only organic materials. Previously, Matyjaszewski group reported a simple and general protocol to

Received: December 2, 2014
Accepted: January 5, 2015
Published: January 8, 2015

DOI: 10.1021/mz500761h
ACS Macro Lett. 2015, 4, 133−137

prepare star (co)polymers consisting of various kinds of arm chains via "arm-first" method using atom transfer radical polymerization (ATRP).[25−27] In "arm-first" method, preformed macroinitiators (arms) are cross-linked by employing a multifunctional coupling reagent such as divinylbenzene (DVB), 1,4-butanediol diacrylate (BDA), and ethylene glycol dimethacrylate (EGDMA). The number of arm in the star (co)polymers can be readily controlled by the ratio of coupling reagent to arms, conversion of coupling reagent, and choice of ligand.

In this work, we designed the neutral star copolymers consisting of poly(styrene-*r*-methyl methacrylate) (PS-*r*-PMMA) random copolymers that can serve as "etching-friendly" additives to control the orientation of microdomains in lamellar forming PS-*b*-PMMA thin films. The star copolymers were synthesized by "arm-first" method using ATRP. We adjusted the composition of styrene and MMA in PS-*r*-PMMA arm chains to find the optimal neutral composition that induce the perpendicular orientation of PS-*b*-PMMA thin films. Consequently, PS-*b*-PMMA thin films containing the star copolymer having 30 mol % styrene and 70 mol % MMA in PS-*r*-PMMA arms show a well-ordered perpendicular orientation after thermal annealing. We also examined the location of neutral star copolymers within the PS-*b*-PMMA thin films by neutron reflectivity using the deuterated star copolymers.

PS-*r*-PMMA based star copolymers were synthesized via arm-first method using ATRP as illustrated in Scheme 1.[26,27]

Scheme 1. Schematic Illustration of Star Copolymer Synthesis by Arm-First Method via ATRP

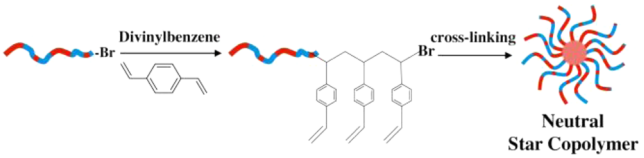

First we synthesized linear random polymers, PS-*r*-PMMA-Br, as arm chains for star copolymers. The composition of styrene and MMA in PS-*r*-PMMA-Br were varied by adjusting the feed mole ratio of styrene and MMA during synthesis, so that the star copolymers have the desired interaction with the PS and PMMA domains of the BCP templates. As a result, PS-*r*-PMMA-Br random polymers have a PS/PMMA composition of 60:40, 50:50, 40:60, 30:70, and 20:80 and they are denoted as arm 6−4, arm 5−5, arm 4−6, arm 3−7, arm 2−8, respectively. The molecular weights (M_ns) of these copolymers were controlled as ∼3000 g/mol. The characteristics of PS-*r*-PMMA random copolymers are summarized in Table 1.

Star copolymers made up with those PS-*r*-PMMA were synthesized by ATRP with divinylbenzene as a cross-linker and they are denoted as star *X*−*Y*, according to the notation of PS-*r*-PMMA-Br arm chains that compose the star copolymers. To remove unreacted linear polymers, the fractional precipitation was performed using dichloromethane as solvent and diethyl ether as nonsolvent.[28] As a consequence, we synthesized the star copolymers consist of a highly cross-linked polyDVB core and PS-*r*-PMMA brush arms. In addition to the relative M_n measured by gel permeation chromatography (GPC), a multiangle light scattering (MALS) method was employed to estimate the absolute M_ns and arm numbers of star copolymers.[25] Comparing to the M_ns from GPC, it was observed that the absolute M_ns from MALS were 3−4 times higher, consistent with the results of Matyjaszewski et al.[26] The absolute M_ns and arm numbers (N_{arm}s) of star copolymers are M_n = ∼170000−340000 g/mol and N_{arm} = ∼40−100, respectively. Also, the hydrodynamic radius (R_h) of star copolymers were measured by dynamic light scattering (DLS) and it was observed that they are in the range R_h = ∼8.8−17.2 nm. The characteristics of star copolymers are also summarized in Table 1.

To investigate the effect of the star copolymers on the PS-*b*-PMMA thin film morphologies, BCP/star copolymer thin films were prepared by spin-casting of 2.0 wt % toluene solutions of 101000 g/mol PS-*b*-PMMA ($f_{PS,volume}$ = 0.53, $Đ$ ∼ 1.10, domain spacing (L_0) ∼ 50.4 nm) with 20 wt % of star copolymers relative to the PS-*b*-PMMA onto pristine silicon substrates. The silicon substrates were not neutralized with PS-*r*-PMMA random copolymer brushes and the film thickness was controlled as ∼75 nm. All samples were then annealed at 200 °C for 4 days in a vacuo. As a control sample, we prepared PS-*b*-PMMA films without star polymers on the silicon substrate. From the optical images of annealed films (Figure S1a), the film exhibits a hole-island (terrace) morphology that clearly indicates the parallel orientation of BCP microdomains (Figure S1b), while the films containing star polymers show the featureless flat surfaces (Figure S2). Furthermore, we also prepared another control sample as PS-*b*-PMMA thin films containing linear PS-*r*-PMMA (M_n = 3700 g/mol) having an optimal neutral PS/PMMA composition of 58:42. As a result, it was shown that the film exhibits the parallel orientation (Figures S1c and S1d), because linear PS-*r*-PMMA chains are dispersed within PS-*b*-PMMA films, thereby not effectively

Table 1. Characteristics of the Synthesized Linear Polymers (Arms) and Star Copolymers

	feed mole ratio in PS-*r*-PMMA		arm		star copolymer					
	styrene	MMA	M_n (g/mol)	$Đ$	M_n[a] (g/mol)	$Đ$[a]	M_n[b] (g/mol)	$Đ$[b]	N_{arm} per star[c]	R_h[d] (nm)
star 6−4	60	40	2600	1.16	78000	1.30	219000	1.39	56	10.2
star 5−5	50	50	3000	1.19	82000	1.34	254000	1.61	59	12
star 4−6	40	60	2700	1.18	91000	1.52	344000	1.62	86	14.7
star 3−7	30	70	3100	1.19	60000	1.30	168000	1.37	38	8.8
star 2−8	20	80	2700	1.18	83000	1.58	423000	1.62	101	17.2
d-star 3−7	30	70	2900	1.18	84000	1.37	331000	1.45	78	14.5

[a]Number-average molecular weight and dispersity measured by GPC in THF with RI detector. [b]Number-average molecular weight and dispersity measured by GPC in THF with MALS detector. [c]The calculation is based on the assumption that all DVB were reacted and were located in the core of star copolymers. [d]Hydrodynamic radius measured by DLS.

DOI: 10.1021/mz500761h
ACS Macro Lett. 2015, 4, 133−137

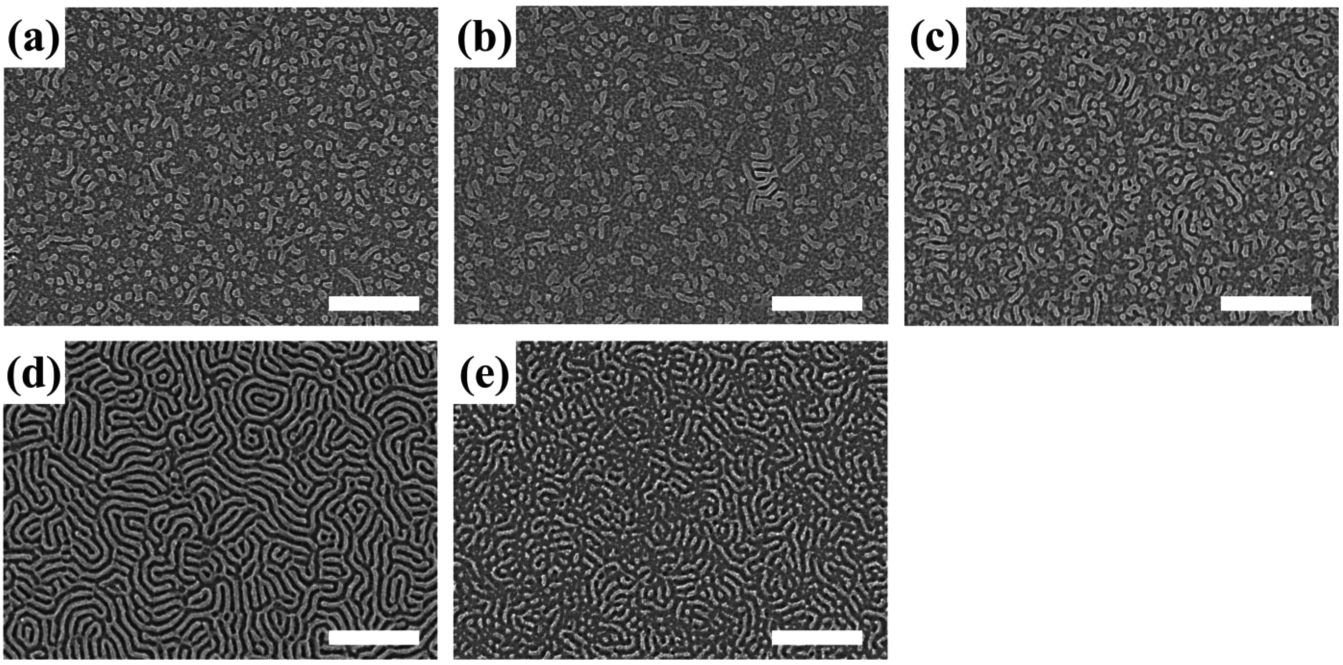

Figure 1. SEM images of 101000 g/mol PS-*b*-PMMA thin films containing 20 wt % of (a) star 6−4, (b) star 5−5, (c) star 4−6, (d) star 3−7, and (e) star 2−8, respectively. Scale bar is 500 nm.

neutralizing the top/bottom interface. Figure 1 represents the scanning electron microscope (SEM) images of PS-*b*-PMMA thin films containing 20 wt % of star 6−4, star 5−5, star 4−6, star 3−7, and star 2−8, respectively. Among these samples, the film with star 3−7 shows the perpendicular orientation in whole area with good ordering whereas the other films show the lower degree of perpendicular orientation and less ordered structures. We also examined the films with star 3−7 as a function of film thickness from ∼1.5 L_0 (75 nm) to ∼2.5 L_0 (127 nm; Figure S3). In this case, it was observed that all films show the perpendicular orientation regardless of film thickness and the perpendicular orientation throughout the film was further confirmed by grazing incidence small-angle X-ray scattering (GISAXS) measurement (Figure S4). It is worth noting that the neutral condition of star copolymer to induce the perpendicular orientation of PS-*b*-PMMA thin films corresponds to the PS and PMMA composition of 30:70 in PS-*r*-PMMA-Br arms, and it is quite different from the well-known neutral composition of PS and PMMA (∼60:40) in PS-*r*-PMMA random copolymers for surface modification.[17,18] We attribute this shifted neutral composition to the cross-linked polyDVB core. The divinylbenzene (DVB) is a styrene-derivative material and hence the chemical property of polyDVB core is similar to that of polystyrene in random copolymers. Therefore, the optimal neutral composition of styrene and MMA in PS-*r*-PMMA-Br is shifted to the higher MMA ratio to compensate the PS-like polyDVB core. The ^{1}H NMR was used to determine the chemical composition of the arms and star copolymers as summarized in Table 2. From ^{1}H NMR spectra of arm 3−7 and star 3−7, it was found that the molar ratio of styrene/MMA in arm 3−7 was 38:62, while the molar ratio of (styrene + DVB)/MMA in star 3−7 was 59:41 and it is different from the feed ratio (Figure S5). In this case, the phenyl protons from polyDVB core showed a weak and broad peak shown from 6 to 8 ppm in ^{1}H NMR spectrum due to the partial immobilization of the cross-linked polyDVB in the star core.[25,29] The value of 59:41 from ^{1}H NMR of star 3−7 is consistent with the neutral composition of PS-*r*-PMMA random copolymers.[15−18]

Table 2. Summary of Feed Mole Ratio and the Composition of Styrene and MMA in PS-*r*-PMMA Arms and the Overall Composition of (Styrene + DVB) and MMA in Star Copolymers Estimated from ^{1}H NMR

	feed mole ratio		composition of PS-*r*-PMMA arm		overall composition	
	sty	MMA	sty	MMA	sty + DVB	MMA
star 6−4	60	40	74	26	82	18
star 5−5	50	50	62	38	75	25
star 4−6	40	60	54	46	71	29
star 3−7	30	70	38	62	59	41
star 2−8	20	80	29	71	48	52

The contents of star copolymers also can be a significant factor to optimize the perpendicular orientation of PS-*b*-PMMA thin films. Figure 2 show the SEM images of 101000 g/mol PS-*b*-PMMA thin films with 10 wt % (9.1 vol %), 20 wt % (16.7 vol %), and 40 wt % (28.6 vol %) of star 3−7, respectively. With 10 wt % of star 3−7, the PS-*b*-PMMA thin film showed partially perpendicular orientation which can be due to an insufficient amount of star copolymers at top surface and bottom interface. The PS-*b*-PMMA thin films containing 20 wt % of star 3−7 exhibited well-ordered perpendicular orientation over a whole area. From our previous study with neutral Au NPs, it was found that only 5 wt % (2.3 vol %) of Au NPs was enough to induce the perpendicular orientation of PS-*b*-PMMA thin films. Such difference can be attributed to an antithetic hardness of particle cores. In general, the neutral particles are located at the intermaterial dividing surfaces (IMDS) between two microdomains due to the balanced enthalpic interactions, and meanwhile, the particles also deform the chain conformation of BCPs near IMDS and cause an entropic penalty. To reduce this entropic penalty in thin films, the particles move

DOI: 10.1021/mz500761h
ACS Macro Lett. 2015, 4, 133−137

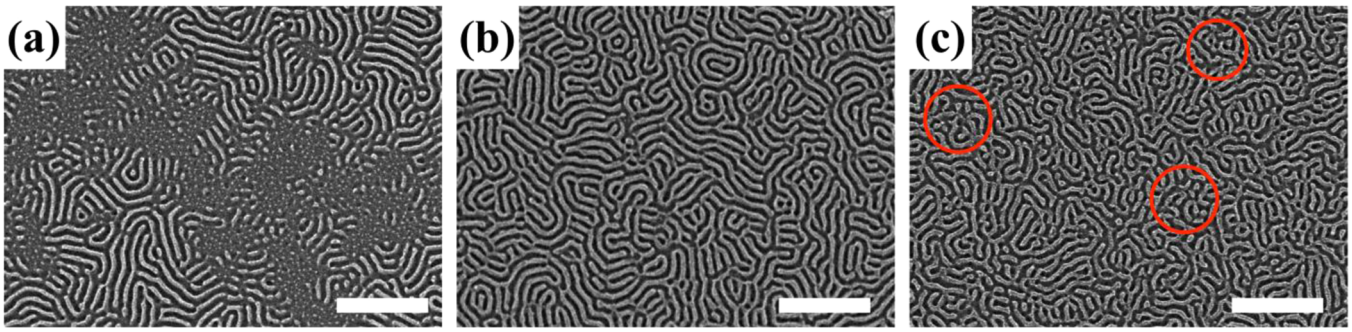

Figure 2. SEM images of 101000 g/mol PS-*b*-PMMA thin films containing (a) 10 wt %, (b) 20 wt %, and (c) 40 wt % of star 3−7, respectively. Scale bar is 500 nm.

toward top surface and bottom interface of the films. However, cross-linked DVB core of star copolymer forms well-known interpenetrating polymer network (IPN) and allows the penetration of BCP chains through the cores. Accordingly, the chain conformation of BCP chains is less changed and the entropic penalty from star copolymers is smaller than that of hard spheres like Au NPs. Therefore, an increased amount of star copolymers with the "soft" core is required to obtain the perpendicular orientation of PS-*b*-PMMA thin films compared to the Au NPs case. With further increasing the amount of star 3−7 to 40 wt %, the thin films still showed the perpendicular orientation but the ordering of microdomains is a little poorer than 20 wt % case (see marked circles in Figure 2c). We attribute a defect of ordering to the excess amount of star copolymers. The excess star copolymers that are mainly located at the IMDS of BCPs can further rumple and fuzz up the PS/PMMA interfaces and distort the lamellar structures as we previously reported.[30] Therefore, it can be concluded that the optimal content of star 3−7 is 20 wt % to induce the perpendicular orientation of PS-*b*-PMMA lamellae without disturbing the BCP microdomains.

Since the trace of PS-*r*-PMMA star copolymers cannot be directly observed by electron microscopy due to the similar chemical structures with PS-*b*-PMMA BCP templates, we employed the neutron reflectivity to examine the location of star copolymers within PS-*b*-PMMA thin films along vertical direction. To provide a contrast between the star copolymers and PS-*b*-PMMA matrix, we used deuterated star copolymers which have much higher scattering length density (SLD) than that of PS-*b*-PMMA. According to the same procedure of arm 3−7 and star 3−7, we synthesized *d*PS-*r*-*d*PMMA-Br with deuterated MMA and styrene, denoted as *d*-arm 3−7 (M_n = 2900 g/mol and $Đ$ = 1.18), and the resulting deuterated star copolymer, denoted as *d*-star 3−7 (M_n = 84000 g/mol and $Đ$ = 1.37). The thin film of 101000 g/mol PS-*b*-PMMA containing 20 wt % of *d*-star 3−7 respect to BCP was prepared onto 4 in. polished silicon wafer (1 mm thick) without any surface treatment and annealed at 200 °C for 4 days in a vacuo. As a control sample, we also prepared BCP films containing linear *d*PS-*r*-*d*PMMA chains, which exhibits the parallel orientation of microdomains (Figure S1). Figure 3 shows the neutron reflectivity profiles and the corresponding SLD profiles of these films. In Figure 3a,b, the solid lines are the best fit to the data based on the model profile along the depth of the film. Calculated SLD values of PS-*b*-PMMA and *d*-star 3−7 composed of *d*PS-*r*-*d*PMMA and hydrogenated DVB are ~1.25 × 10^{-6} Å^{-2} and ~4.2 × 10^{-6} Å^{-2}, respectively, exhibiting high contrast of SLD between them. Therefore, the high SLD

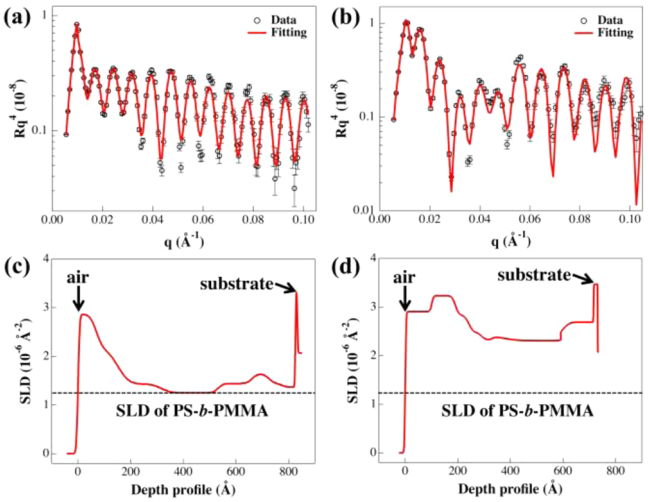

Figure 3. (a) Neutron reflectivity and (c) the corresponding scattering length density profiles of 101 000 g/mol PS-*b*-PMMA thin film containing 20 wt % of *d*-star 3−7 and (b) neutron reflectivity and (d) the corresponding scattering length density profiles of 101000 g/mol PS-*b*-PMMA thin film containing 40 wt % of linear *d*PS-*r*-*d*PMMA chains. The scattering length density profiles are obtained from fitting the reflectivity data (solid line).

regions indicate the segregation of the *d*-star 3−7 star copolymers from the SLD profile in Figure 3c, where the *d*-star 3−7 are mainly observed at the top (polymer/air interface) surface and bottom (polymer/substrate interface) surface. It should be noted that the top/bottom segregation is also observed in other nonlinear architecture systems, such as bottlebrush or branched polymers within linear polymer films.[31,32] In contrast, the neutron reflectivity profile and calculated SLD profile in Figure 3b,d clearly indicate that linear chains are dispersed within PS-*b*-PMMA films with slight segregation at the top and bottom of the film. This result also supports that the neutral star copolymers prefer to segregate at the top and bottom surface to reduce the entropic penalty due to their bulky size and highly grafted arms, thereby effectively inducing the perpendicular orientation of PS-*b*-PMMA lamellae.

In summary, we designed the neutral star copolymers as etching-friendly additives to BCP thin films to control the orientation of microdomains without any surface modification. Star copolymers consisting of PS-*r*-PMMA arms and cross-linked polyDVB core were synthesized by arm-first method via ATRP technique, and the chemical properties of star copolymers are precisely tuned by varying the composition of

DOI: 10.1021/mz500761h
ACS Macro Lett. 2015, 4, 133−137

styrene and MMA in PS-*r*-PMMA arms to optimize the neutral condition of star copolymers within PS-*b*-PMMA thin films. As a result, the well-ordered perpendicular orientation of PS-*b*-PMMA lamellae was observed when incorporating star 3−7, which have an overall composition of PS and PMMA with 59:41, very close to the neutral composition of conventional PS-*r*-PMMA random copolymer brushes. Furthermore, the location of star copolymers were examined with neutron reflectivity by employing deuterated star copolymers. In this case, it was observed that the star copolymers are mainly segregated at the top and bottom surfaces within the PS-*b*-PMMA thin films along vertical direction. To reduce the entropic penalty, the neutral star copolymers move to the top and bottom of the films and thus they neutralize the surface and substrate, leading to the perpendicular orientation of BCP microdomains. Our method may provide a facile way to prepare well-defined BCP nanopatterns with etching-friendly templates without an aid of any additional surface modification steps, which can further enrich the applicability of BCP patterns regardless of substrates.

■ ASSOCIATED CONTENT

Supporting Information

Experimental methods and additional NMR data. This material is available free of charge via the Internet at http://pubs.acs.org.

■ AUTHOR INFORMATION

Corresponding Authors

*E-mail: jgson@kist.re.kr.
*E-mail: joona@korea.ac.kr.

Notes

The authors declare no competing financial interest.

■ ACKNOWLEDGMENTS

This work was by National Research Foundation of Korea grant funded by the Korea government (MSIP; Nos. 2012R1A2A2A01014473, 2012M3A7B4049863, 2014M2B2A4031763, and 2012M3A7B4035323) and also by the Global Frontier R&D Program (No. 2013M3A6B1078869) on Center for Hybrid Interface Materials (HIM) funded by the Ministry of Science, ICT & Future Planning. J.G.S. acknowledges the support by Korea Institute of Science & Technology (KIST) internal project.

■ REFERENCES

(1) Bang, J.; Jeong, U.; Ryu, D. Y.; Russell, T. P.; Hawker, C. J. *Adv. Mater.* **2009**, *21*, 4769−4792.
(2) Hawker, C. J.; Russell, T. P. *MRS Bull.* **2005**, *30*, 952−966.
(3) Phillip, W. A.; O'Neill, B.; Rodwogin, M.; Hillmyer, M. A.; Cussler, E. L. *ACS Appl. Mater. Interfaces* **2010**, *2*, 847−853.
(4) Hong, A. J.; Liu, C. C.; Wang, Y.; Kim, J.; Xiu, F. X.; Ji, S. X.; Zou, J.; Nealey, P. F.; Wang, K. L. *Nano Lett.* **2010**, *10*, 224−229.
(5) Kim, M.; Safron, N. S.; Han, E.; Arnold, M. S.; Gopalan, P. *Nano Lett.* **2010**, *10*, 1125−1131.
(6) Fan, H. J.; Werner, P.; Zacharias, M. *Small* **2006**, *2*, 700−717.
(7) Jung, H.; Hwang, D.; Kim, E.; Kim, B. J.; Lee, W. B.; Poelma, J. E.; Kim, J.; Hawker, C. J.; Huh, J.; Ryu, D. Y.; Bang, J. *ACS Nano* **2011**, *5*, 6164−6173.
(8) Anastasiadis, S. H.; Russell, T. P.; Satija, S. K.; Majkrzak, C. F. *Phys. Rev. Lett.* **1989**, *62*, 1852−1855.
(9) Coulon, G.; Russell, T. P.; Deline, V. R.; Green, P. F. *Macromolecules* **1989**, *22*, 2581−2589.
(10) Bang, J.; Kim, S. H.; Drockenmuller, E.; Misner, M. J.; Russell, T. P.; Hawker, C. J. *J. Am. Chem. Soc.* **2006**, *128*, 7622−7629.
(11) Kim, S. H.; Misner, M. J.; Xu, T.; Kimura, M.; Russell, T. P. *Adv. Mater.* **2004**, *16*, 226−231.
(12) Thurn-Albrecht, T.; DeRouchey, J.; Russell, T.; Jaeger, H. *Macromolecules* **2000**, *33*, 3250−3253.
(13) Sivaniah, E.; Hayashi, Y.; Iino, M.; Hashimoto, T.; Fukunaga, K. *Macromolecules* **2003**, *36*, 5894−5896.
(14) Kim, T.; Wooh, S.; Son, J. G.; Char, K. *Macromolecules* **2013**, *46*, 8144−8151.
(15) Bang, J.; Bae, J.; Löwenhielm, P.; Spiessberger, C.; Given-Beck, S. A.; Russell, T. P.; Hawker, C. J. *Adv. Mater.* **2007**, *19*, 4552−4557.
(16) Jung, H.; Leibfarth, F. A.; Woo, S.; Lee, S.; Kang, M.; Moon, B.; Hawker, C. J.; Bang, J. *Adv. Funct. Mater.* **2013**, *23*, 1597−1602.
(17) Mansky, P.; Liu, Y.; Huang, E.; Russell, T.; Hawker, C. *Science* **1997**, *275*, 1458−1460.
(18) Ryu, D. Y.; Shin, K.; Drockenmuller, E.; Hawker, C. J.; Russell, T. P. *Science* **2005**, *308*, 236−239.
(19) Bates, C. M.; Seshimo, T.; Maher, M. J.; Durand, W. J.; Cushen, J. D.; Dean, L. M.; Blachut, G.; Ellison, C. J.; Willson, C. G. *Science* **2012**, *338*, 775−779.
(20) Kim, E.; Kim, W.; Lee, K. H.; Ross, C. A.; Son, J. G. *Adv. Funct. Mater.* **2014**, *24*, 6981−6988.
(21) Son, J. G.; Bulliard, X.; Kang, H.; Nealey, P. F.; Char, K. *Adv. Mater.* **2008**, *20*, 3643−3648.
(22) Ji, S.; Liu, C.-C.; Liu, G.; Nealey, P. F. *ACS Nano* **2010**, *4*, 599−609.
(23) Yoo, M.; Kim, S.; Jang, S. G.; Choi, S.-H.; Yang, H.; Kramer, E. J.; Lee, W. B.; Kim, B. J.; Bang, J. *Macromolecules* **2011**, *44*, 9356−9365.
(24) Balazs, A. C.; Emrick, T.; Russell, T. P. *Science* **2006**, *314*, 1107−1110.
(25) Gao, H. F.; Tsarevsky, N. V.; Matyjaszewski, K. *Macromolecules* **2005**, *38*, 5995−6004.
(26) Gao, H.; Matyjaszewski, K. *J. Am. Chem. Soc.* **2007**, *129*, 11828−11834.
(27) Xia, J. H.; Zhang, X.; Matyjaszewski, K. *Macromolecules* **1999**, *32*, 4482−4484.
(28) Hazer, B.; Baysal, B. M. *Polymer* **1986**, *27*, 961−968.
(29) Spěváček, J. *Makromol. Chem., Rapid Commun.* **1982**, *3*, 697−703.
(30) Kim, S.; Yoo, M.; Kang, N.; Moon, B.; Kim, B. J.; Choi, S.-H.; Kim, J. U.; Bang, J. *ACS. Appl. Mater. Interfaces* **2013**, *5*, 5659−5666.
(31) Mitra, I.; Li, X.; Pesek, S. L.; Makarenko, B.; Lokitz, B. S.; Uhrig, D.; Ankner, J. F.; Verduzco, R.; Stein, G. E. *Macromolecules* **2014**, *47*, 5269−5276.
(32) Lee, J. S.; Lee, N. H.; Peri, S.; Foster, M. D.; Majkrzak, C. F.; Hu, R.; Wu, D. T. *Phys. Rev. Lett.* **2014**, *113*, 225702.

DOI: 10.1021/mz500761h
ACS Macro Lett. 2015, 4, 133−137